Geological Quarterly, 2023, 67: 15
DOI: http://dx.doi.org/10.7306/gq.1685

Palaeobiogeography, palaeoecology, and sequence stratigraphy of the Upper Jurassic carbonate succession of the Lar Formation, central Alborz Zone, Iran

Zahra SALEH[1, *] and Daniela REHÁKOVÁ[2]

[1] Kharazmi University, Department of Geology, Faculty of Earth Science, Tehran, Iran; ORCID: 0000-0003-0031-5347

[2] Comenius University, Department of Geology and Paleontology, Faculty of Natural Sciences, Ilkovičova 6, 84215 Bratislava, Slovakia; ORCID: 0000-0002-3569-9179

Saleh, Z., Reháková, D., 2023. Palaeobiogeography, palaeoecology, and sequence stratigraphy of the Upper Jurassic carbonate succession of the Lar Formation, central Alborz Zone, Iran. Geological Quarterly, 2023, 67: 15, doi: 10.7306/gq.1685

Associate Editor: Jacek Grabowski

Foraminifera, ammonites, and calcareous dinoflagellates were used for stratigraphy and, together with microfacies, for the assessment of the palaeoenvironmental conditions of the Upper Jurassic deposits in the central Alborz Zone of northern Iran. The Lar Formation (Lar Fm.) in the Polur section is of latest Oxfordian to early Kimmeridgian age. The ammonite *Subnebrodites planula* and the calcareous dinoflagellate *Colomisphaera nagyi* have been introduced as new biomarkers of the lower Kimmeridgian in the central Neo-Tethys. The distribution of calcareous dinoflagellates reflects possible dispersal routes along a narrow seaway between the western Neo-Tethys and the Alborz Zone in the central Neo-Tethys. The *Terebella-Crescentiella* associations of the Lar Fm. represent a low-energy setting under dysoxic conditions in the Central Neo-Tethys Ocean. The benthic foraminiferal assemblages in this formation show a high dominance of infaunal taxa and r-selected strategists. This assemblage is reminiscent of eutrophic conditions and low oxygen levels in the lower part of the Lar Fm. Good preservation of the hexactinellid sponges in the upper part of the Lar Fm. also indicates an oxygen-minimum zone. Three third-order depositional sequences can be distinguished in the study area based on six microfacies. Depositional sequence 1 (DS1) is composed mainly of argillaceous limestone and medium- to thick-bedded limestone, corresponding to an outer ramp-to-middle ramp environment. Depositional sequence 2 (DS2) comprises breccia limestone and thick-bedded limestone facies in its lower part and thin-bedded limestone to massive limestone in its upper part. The breccia limestone facies may be associated with subaerial exposure and reworking of previously deposited sediment during a relative sea level fall. The thin-bedded limestone to massive limestone of DS2 consists mainly of bioclastic mudstone to wackestone (outer ramp). These represent an deep-water outer homoclinal ramp facies. Depositional sequence 3 (DS3) consists mainly of massive limestone to thick-bedded limestone with a bioclastic peloidal microbial *Crescentiella* packstone (middle ramp). The relative stratigraphic positions of DSs1–3 and sequence boundaries in the uppermost Oxfordian to lower Kimmeridgian of the Polur area show a fair match to the upper Oxfordian to lower Kimmeridgian sequences (JOx7, JOx8, JKi1 and JKi2) on the global sea level curve.

Key words: Upper Jurassic, microfacies, foraminifera, ammonites, calcareous dinoflagellates, biostratigraphy, sequence stratigraphy, Alborz Zone, Iran.

INTRODUCTION

The Late Jurassic interval represents a period of major sea level fluctuations in the Neo-Tethys Ocean (Gerdes et al., 2010). The global sea level curve by Haq (2018) reveals a long-term transgression from the Bajocian/Bathonian transition to the late Kimmeridgian/early Volgian. Gradstein et al. (2017) suggested that the sea level in the Late Jurassic was 80 or more metres higher than the present level, reflecting rifting in the Central Atlantic and producing abundant deep-water facies in marine sequences. Ammonites, calcareous dinoflagellates and planktonic and benthic foraminifera were widely distributed fossil groups of the Neo-Tethys Ocean in the Late Jurassic and have considerable stratigraphic importance (Moliner and Olóriz, 2009; Reháková et al., 2011; Sarfi and Yazdi-Moghadam., 2016; Gradstein et al., 2017). Our research provides new biomarkers and new insights into the stratigraphy and detailed characteristics of ammonites and calcareous dinoflagellates in the Upper Jurassic of the central Neo-Tethys. In our study, agglutinated and planktonic foraminifera, micro-encruster associations and hexactinellid sponges are used as indicators of palaeobathymetry and/or organic carbon flux, while biotic and sedimentary proxies help assess changing depositional conditions. Marine Upper Jurassic limestones (Lar Fm.) are widely distributed in northern Iran within the Alborz Zone (Fig. 1A) and enable study of the distribution of microfauna and microfacies

* Corresponding author, e-mail: saleh.zahra.khu@gmail.com

Received: August 10, 2022; accepted: March 16, 2023; first published online: 26 July, 2023

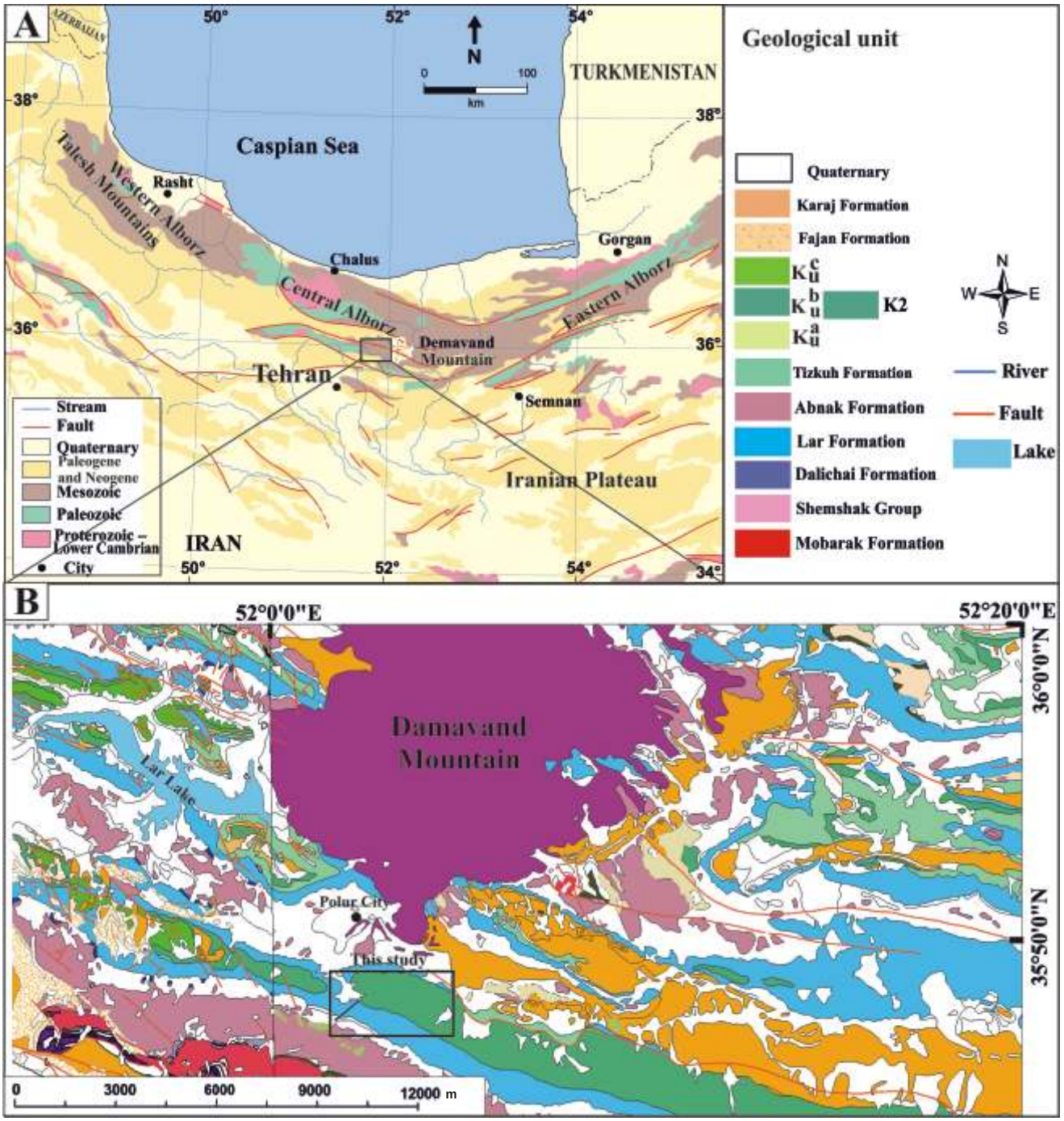

Fig. 1A – geological map of the Alborz Zone showing the distribution of the Mesozoic deposits (modified after Muttoni et al., 2009); B – geological context for the Polur section of the Lar Fm. and K2 rock unit in the Alborz Zone, north Iran (modified after Vahdati-Daneshmand, 1997)

that can then be placed in a sequence-stratigraphic framework. While many previous studies have focused on the palaeontological and stratigraphic aspects of the Upper Jurassic deposits (Lar Fm.) of the north of Iran (e.g., Assereto, 1966; Seyed-Emami et al., 1995; Naderi, 2002; Majidifard, 2008; Aghaei et al., 2012; Daneshian and Saleh, 2020), only a few detailed investigations on sedimentology and sequence stratigraphy have been attempted (Fathi and Mosaddegh, 2012; Daneshian et al., 2021). However, study of the depositional facies and the sequence-stratigraphic framework improve knowledge of the Lar Fm., and generally of the Upper Jurassic deposits in the Middle East. The objectives of this research are:

– to refine the biostratigraphy of the Jurassic deposits in the central Neo-Tethys by means of planktonic and benthic agglutinated foraminifera, ammonites, and calcareous dinoflagellate cysts;
– to document the changes in the benthic and planktonic foraminiferal associations, micro-encruster associations, and sponges as a result of changes in environmental conditions;
– to define a sequence-stratigraphic framework for the Upper Jurassic deposits in the central Neo-Tethys.

GEOLOGICAL SETTING

GENERAL GEOLOGY

According to Stöcklin (1968), Iran can be divided into a number of zones (the Kopet-Dagh Zone, the Makran and eastern Iran Zones, the Alborz Zone, the Zagros Zone, the Sanandaj-Sirjan Zone, the Lut Block, the Urumieh-Dokhtar Zone, and Central Iran). One section, at Polur (35°48'38"N, 52°03'19"E) was chosen for assessment of changing depositional conditions in the Upper Jurassic deposits (Lar Fm.) of the central Neo-Tethys. The Polur section is located near the city of Polur in the central part of the Alborz Zone, south of Mount Damavand and ~88 km north-east of Tehran (Fig. 1B). The Polur section includes an inclined syncline axis and a fault that cuts the Upper Jurassic strata. The Alborz Zone, northern Iran, is a chain of mountains along the southern side of the Caspian Sea that was produced by the collision of Iran with Eurasia (Zanchi et al., 2006). The northern boundary of the Alborz Zone coincides with the southern side of the Caspian Basin (Barrier and Vrielynck, 2008). There is no clear boundary in the south of the Alborz Zone, and the transition from central Iran to the Alborz plate is gradual (Barrier and Vrielynck, 2008). This zone has a length of ~600 km and a width of 100 km and extends from the Talesh Mountains in northwestern Iran to the Binaloud Mountains in the north-east (Barrier and Vrielynck, 2008).

GEODYNAMIC SETTING OF THE ALBORZ ZONE DURING THE LATE JURASSIC

During the Late Jurassic, the Lar Fm. was deposited in a ramp environment (Daneshian et al., 2021), but during the Tithonian and Berriasian (Fig. 2), the sea retreated and the first major tectonic uplift associated with the Late Cimmerian orogeny occurred (Aghanabati, 2004; Daneshian et al., 2021). The Late Cimmerian tectonic event was triggered by a back-arc rift system on the Cimmerian microcontinent (Bochud, 2011). This event created major faults and fractures in the Lar Fm. (Aghanabati, 2004; Daneshian et al., 2021); it coincides with inversion of the Alborz Mountains (Shahidi et al., 2008).

METHODS

A total of one hundred and seventy-three samples were collected from 450 m of the Upper Jurassic deposits of the Lar Fm. and the Dalichai Formation (Dalichai Fm.) with a sampling distance of 2–3 m. The illustrations and definitions of Loeblich and Tappan (1988), Reháková (2000a, b), Reháková et al. (2011), Majidifard (2008), Schweigert and Kuschel (2017), Bakhmutov et al. (2018) and Kowal-Kasprzyk et al. (2020) were used for the determination of foraminifera, dinoflagellate cysts, and ammonites. The textures of the carbonate deposits were described using the classifications of Dunham (1962), Embry and Klovan (1971) and Wright (1992). Interpretations of microfacies and depositional environments are based on Flügel (2010). Relative sea level variations have been interpreted based on changes in microfacies and depositional environment based on standard facies classifications (e.g., Wilson, 1975; Flügel, 2010). Data from these studies were then used to delineate a sequence-stratigraphic framework using criteria described by Hunt and Tucker (1992, 1995) and Catuneanu et al. (2011). Palaeoecological methods include the use of agglutinated and calcareous foraminifera morphogroups. The agglutinated foraminiferal morphogroup scheme used in the study is mostly based on the work of Jones and Charnock (1985), Cetean et al. (2011) and Nagy and Hendrickson (2022).

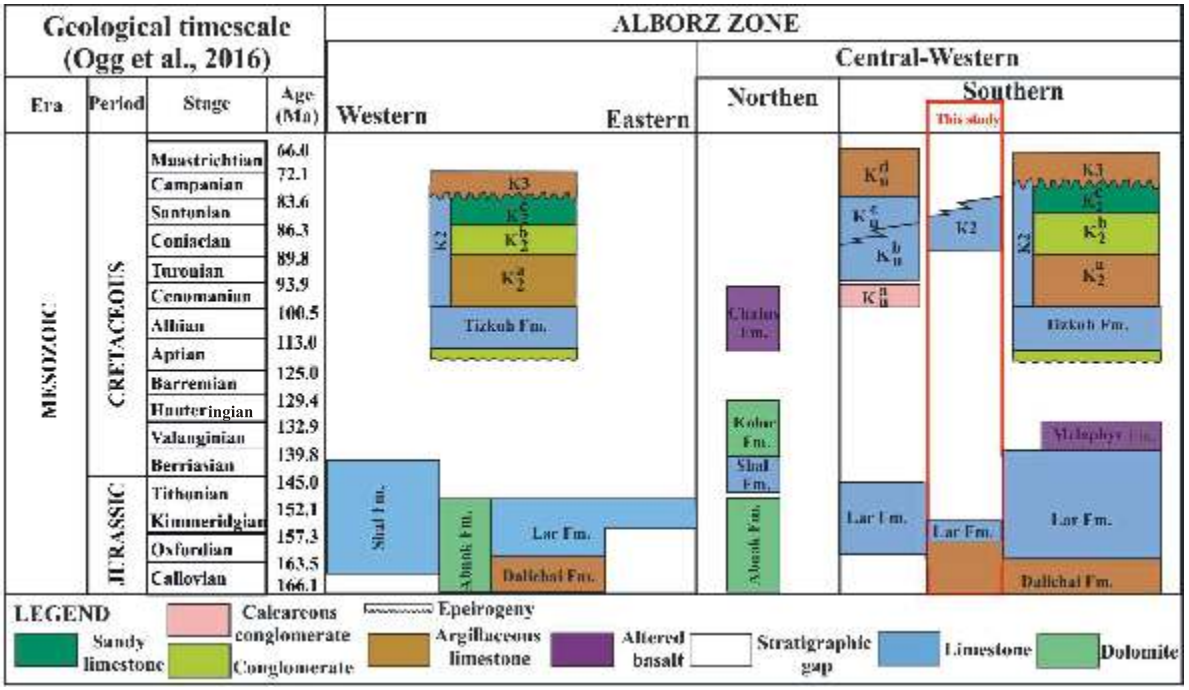

Fig. 2. Chronostratigraphic chart (after Ogg et al., 2016) and stratigraphic columns of the Upper Triassic to Upper Cretaceous of the Alborz Zone (modified after Aghanabati and Rezaie, 2009)

RESULTS

LITHOSTRATIGRAPHY

The type section of the Lar Fm. was first described by Assereto (1966) from the north-east of Garmabdar village, central Alborz Zone, northern Iran, though so far it has not been measured. According to Assereto (1966), the age of the Lar Fm. is Oxfordian to Kimmeridgian based on ammonites. The main sedimentary environments of this formation were marine carbonate platforms and ramps.

In stratigraphic order, the Polur section consists of the Shemshak Group (Upper Triassic to Lower Jurassic), the Dalichai Fm. (Middle to Upper Jurassic), the Lar Fm. (uppermost Oxfordian to lower Kimmeridgian), and the K2 rock unit (middle-upper Coniacian to Santonian?; Figs. 2 and 4). The Lar Fm. conformably overlies the Dalichai Fm. (Fig. 3A). The boundary between these two formations has been drawn between the marly limestone level of the Dalichai Fm. (Fig. 3B), which is rich in ammonites (Fig. 3D–F), and the medium-bedded limestone level of the Lar Fm with common chert nodules (Fig. 3A, C). The Lar Fm. is ~390 m thick and is informally subdivided into a "lower unit" characterized by alternating medium-bedded and thick-bedded limestone along with breccia limestone, chert nodules and karstification, a "middle unit" that is dominated by thin-bedded limestone, and an "upper unit" consisting of massive and thick-bedded limestone along with chert nodules and pervasive karstification (Fig. 4C). The upper and lower units of the Lar Fm. have been affected by various diagenetic and tectonic processes such as cementation, dissolution, fracturing, dolomitization, and dedolomitization. The middle unit of the Lar Fm. shows less diagenesis compared to the upper and lower parts of the Lar Fm. The uppermost part of the Lar Fm. is faulted and the boundary with the K2 rock unit has been drawn where this fault is located (Fig. 4B).

BIOSTRATIGRAPHY

The microfossils of the Polur section include mainly planktonic and benthic foraminifera, skeletal fragments of *Saccocoma* planktonic crinoids, calcareous dinoflagellate cysts and *Bositra* microfilaments. The microfossils are generally poorly preserved in the Lar Fm. due to severe epigenic karstification and significant tectonic activity. However, in the Polur section, we found several foraminifera (*Ammobaculites*, *Bullopora*, *Eomarssonella, Reophax*, *Globuligerina oxfordiana*). The benthic foraminifera documented do not offer a high-resolution zonation, a consequence of the slow rate of evolution of benthic foraminifera and the lack of a continuous planktonic foraminifera record. However, within the Alborz Zone, the distribution of the foraminifera provides a fair basis for biostratigraphy (Sarfi and Yazdi-Moghadam, 2016). To improve the biostratigraphy, ammonites have also been used in this research because Jurassic ammonites allow effective biostratigraphic zonation and correlation in the lower Kimmeridgian (Moliner and Olóriz, 2009).

Based on the foraminifera, ammonites and calcareous dinoflagellate cysts, the age of strata of the upper part of the Dalichai and the Lar formations can be attributed to the late Oxfordian to early Kimmeridgian (Figs. 5 and 6).

UPPERMOST OXFORDIAN-KIMMERIDGIAN

Globuligerina oxfordiana, a planktonic foraminiferal species, has been recorded in argillaceous limestone at the top of the Dalichai Fm. (Figs. 5A–E and 6) and the base of the Lar Fm. *Globuligerina oxfordiana* commonly occurs in the Bajocian through the early Tithonian interval (Gradstein et al., 2017). In Iran and Syria (Kuznetsova et al., 1996), *Globuligerina oxfordiana* has been recorded in uppermost Oxfordian strata and usually is encountered at the top of the Dalichai Fm. (Majidifard, 2008). In the Polur area, *Orthosphinctes*, which indicates an Oxfordian-Kimmeridgian age, occurs in the uppermost of the Dalichai Fm., very close to the boundary between the Dalichai and the Lar formations (Fig. 3F); therefore, based on these two fossils, we attribute a latest Oxfordian-earliest Kimmeridgian age to the top of the Dalichai Fm. and the base of the Lar Fm.

LOWER KIMMERIDGIAN

The base of the Lar Fm. is marked by the disappearance of *Globuligerina oxfordiana*. The ammonite species *Subnebrodites planula,* the index species for the early Kimmeridgian Planula Zone (Schweigert and Kuschel, 2017), has been found at the top of the Lar Fm., very close to the boundary between the Lar Fm. and the K2 rock unit (Figs. 4A and 5N); therefore, the age of the Lar Fm. is latest Oxfordian-earliest Kimmeridgian at the base, and early Kimmeridgian at the top of the formation. *Colomisphaera nagyi* as a calcareous dinoflagellate has been found above *Globuligerina oxfordiana* in the lower part of the Lar Fm. The first occurrence of *Colomisphaera nagyi* has been documented from upper Kimmeridgian deposits (Reháková, 2000a; Ivanova, et al., 2008); therefore, the potential first appearance of *Colomisphaera nagyi* in the Polur section during the early Kimmeridgian could be significant (Fig. 5F, G). The occurrence of the early Kimmeridgian Planula Zone in the upper part of the Lar Fm. and above *Colomisphaera nagyi* indicates that the species *Colomisphaera nagyi* was already present in the early Kimmeridgian. On the other hand, traditionally in the Upper Jurassic deposits of Iran, the foraminifer *Alveosepta jaccardi* has been used as an indicator of the late Oxfordian-early Kimmeridgian time interval (Sarfi and Yazdi-Moghadam, 2016). In the Polur section, *Alveosepta jaccardi* has not been documented, probably due to stressful environmental conditions that prevailed during the deposition of the Lar Fm. Smaller benthic foraminifera, however, can successfully thrive in a stressful environment (Sarfi and Yazdi-Moghadam, 2016). *Ammobaculites, Bullopora*, *Eomarssonella* and *Reophax* have been identified (Fig. 5H–J) above *Colomisphaera nagyi.* Elsewhere in Iran, these are commonly associated with *Alveosepta jaccardi* and therefore support an early Kimmeridgian age.

MICROFACIES AND DEPOSITIONAL ENVIRONMENT

Microfacies is defined as "...the totality of all sedimentological and palaeontological data that can be described and classified from thin-sections..." (Flügel, 2010). In the study area, depositional textures were used to delineate six microfacies (MF), based on which associated depositional environments within the Lar Fm. were defined (Fig. 7).

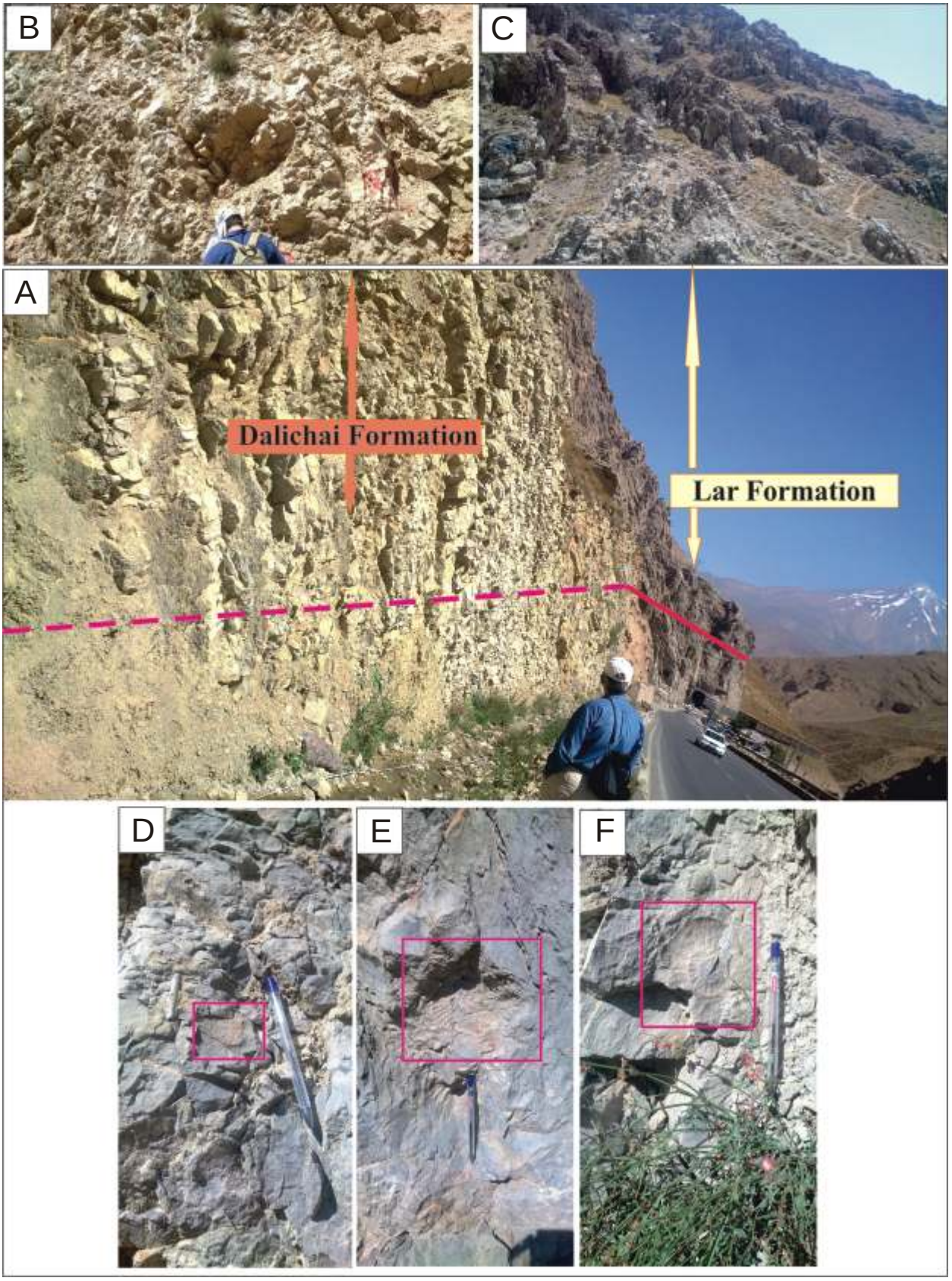

Fig. 3A – Nature of the contact of the Dalichai Fm. with the overlying Lar Fm., Polur area; the contact can be distinguished in the field by changes in lithology from marly limestone to medium-bedded limestone; the upper part of the Dalichai Fm. is marked by a dashed pink line and the lower part of the Lar Fm. is marked by a solid red line; B – an overview of the upper part of the Dalichai Fm.; C – an overview of the lower part of the Lar Fm.; D, E – uppermost Oxfordian-lowest Kimmeridgian? ammonite in the Dalichai Fm.; F– *Orthosphinctes* close to the boundary between the Dalichai and Lar formations

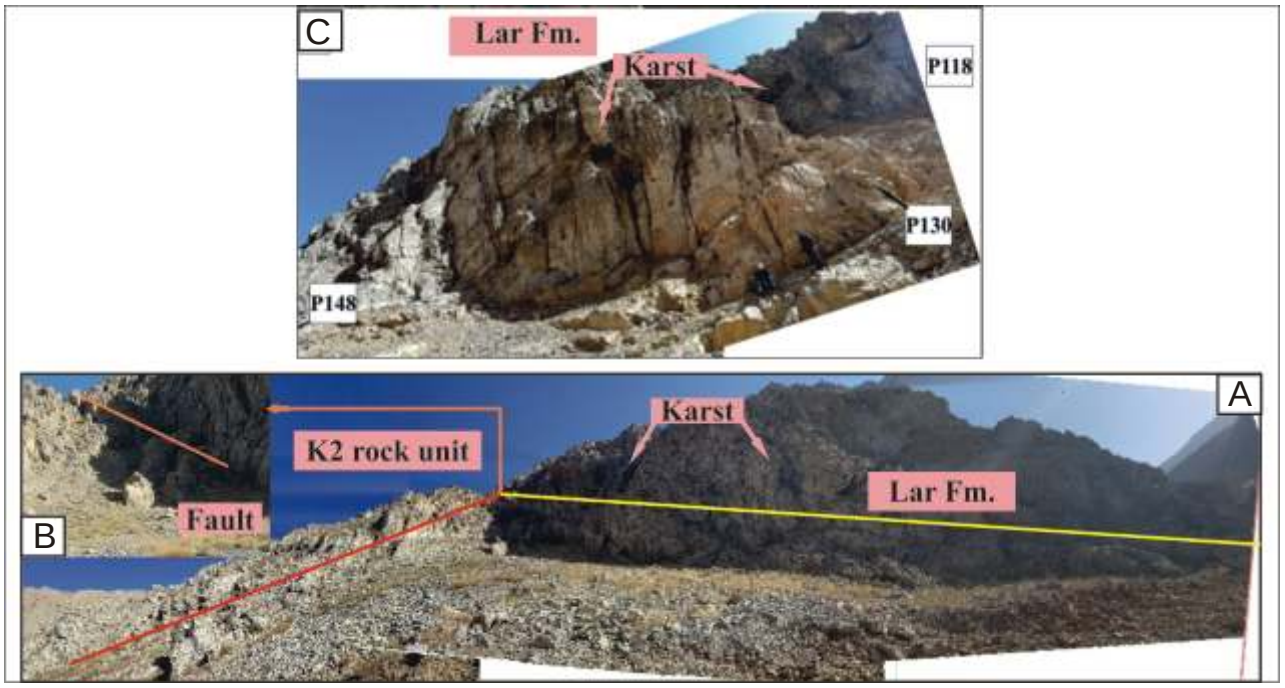

Fig. 4A – an overview of the Kimmeridgian limestone in the Lar Fm.; the upper part of the Lar Fm. is marked by a solid yellow line and the lower part of the K2 rock unit is marked by a solid red line; B – close-up views of the boundary between the Lar Fm. and K2 rock unit in the Polur section; the boundary between the Lar Fm. and K2 rock units is marked by a solid orange line and a fault; C – karst cavities in the uppermost part of the Lar Fm.

MF-A, DOLOMITIC SPARSTONE (MIDDLE RAMP)

Dolomite is structurally destructive and largely modifies earlier features. Based on the size of crystals and crystal boundaries in the Polur section, three replacement dolomite textures were recognized (Fig. 7A1–A6). Replacive dolomite 1 (RD1) forms small (40–100 μm) euhedral crystals with planar crystal boundaries that replace the original ones. This type of dolomite displays a red colour if viewed with cathodoluminescence (CL) microscopy (Fig. 7A3). Replacive dolomite 2 (RD2) forms small to medium-sized (40–250 μm) euhedral crystals that replace a large amount of the original rock fabric. Crystal borders show bright orange luminescent rims under CL microscopy (Fig. 7A4) but the crystal centres show red luminescence. Replacive dolomite 3 (RD3) forms medium to coarse (250–300 μm) euhedral to anhedral crystals that replace preexisting limestone or are a product of recrystallization of earlier formed dolomite (Fig. 7A5). Crystal borders show bright orange luminescent rims under CL microscopy. Their distribution is closely related to unconformities, being located near sequence boundaries.

Taking into account the findings of Daneshian et al. (2021) that dolomitic sparstone of the Lar Fm. in the Marghsso section was formed in a mid-ramp environment in high-energy conditions, it can be inferred that the dolomites in the study area belong to a high-energy and mid-ramp carbonate platform. Besides, this microfacies is located close to a microbial association and there is no evidence of a lagoonal environment. Kýrmacý (2013) showed that replacive dolomites were formed at shallow-intermediate burial depths.

MF-B, INTRACLASTIC BIOCLASTIC WACKESTONE TO PACKSTONE (MIDDLE RAMP)

This microfacies is characterized by abundant intraclasts (carbonate sediment that has been eroded, redeposited, and derived from other microfacies) and bioclasts including fragments of brachiopods, ostracods, bivalves, bryozoans, foraminifera, recrystallized radiolarians and rare microbial encrustations. Dolomite can be observed locally (Fig. 7B). The surfaces of subangular intraclasts are commonly coated by microbial envelopes. A cyst of *Colomisphaera nagyi* was found in this microfacies.

MF-C, BIOCLASTIC PELOIDAL MICROBIAL *CRESCENTIELLA* PACKSTONE TO GRAINSTONE (MIDDLE RAMP)

This microfacies contains abundant detrital material bound by microbialites, with ubiquitous fragments of *Crescentiella morronensis* accompanied by *Terebella lapilloides*, coated grains and abundant peloids (Fig. 7C1). The peloids are characterized by different sizes, occurring irregularly in packstone to grainstone textures and contributing to microbial associations. The oncoids are characterized by large sizes in packstone to grainstone textures and are associated with *Crescentiella morronensis*. Bioclastic elements include bryozoans, echinoids, crinoids, brachiopods, sponges, recrystallized radiolarians and benthic foraminifera (*Reophax*). In places, sponge-microbial floatstones can be observed where peloids are less abundant than sponges (Fig. 7C2). *Crescentiella morronensis* produced a "robust" (Figs. 7C and 8G) thick wall typical of shallow-water conditions (Leinfelder, 2001).

MF-D, BIOCLASTIC MICROBIAL PELOIDAL PACKSTONE TO GRAINSTONE (MIDDLE RAMP)

Calcified sponges, brachiopod fragments, echinoids and bryozoans are observed within this microfacies. Abundant peloids and a few microbial organisms (*Terebella* and *Crescentiella*) are other associated non-skeletal grains (Fig. 7D). The peloids are characterized by different sizes, irregularly

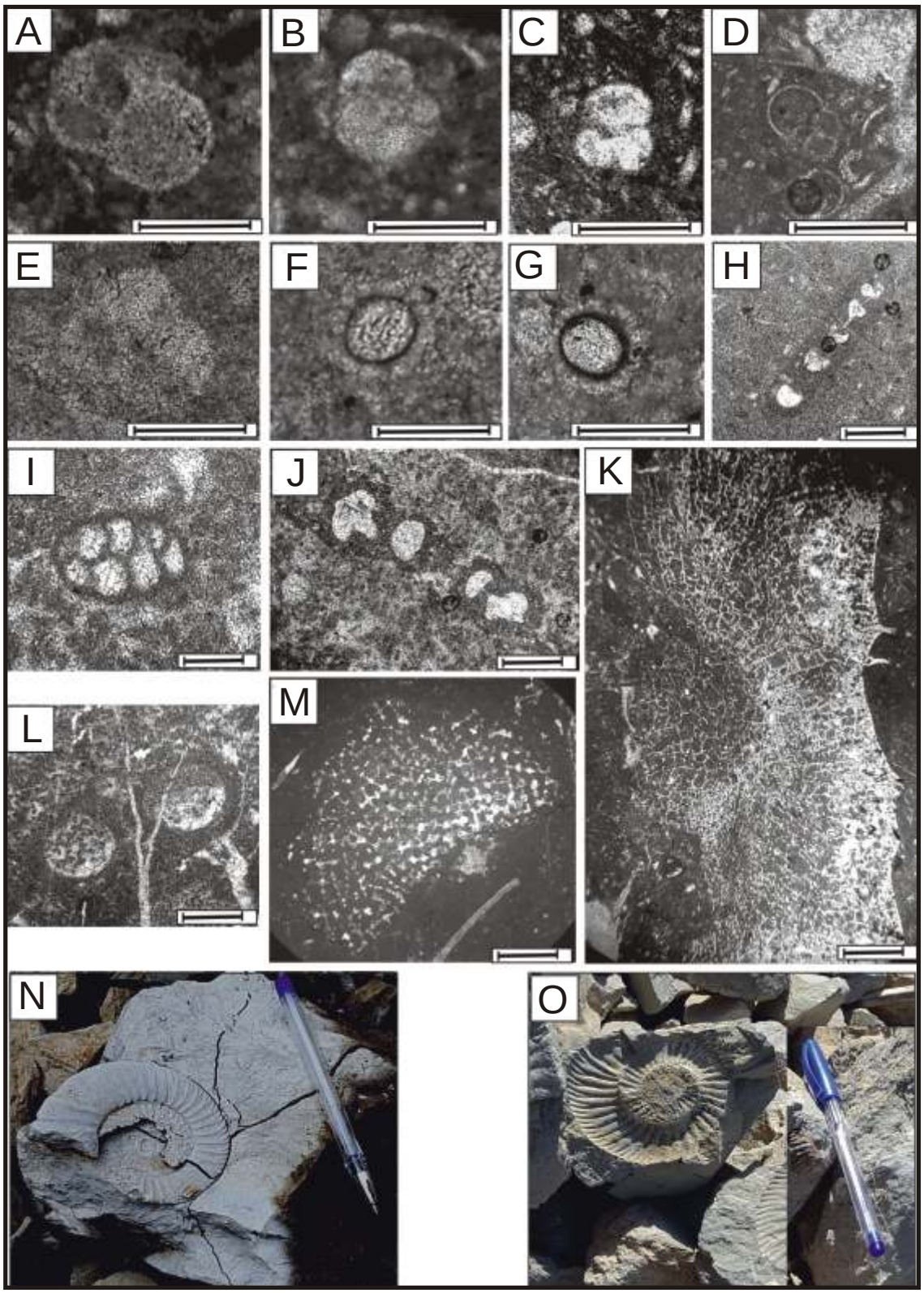

Fig. 5A–D – *Globuligerina oxfordiana* (Grigelis) sample no. 14; E – *Globuligerina oxfordiana* (Grigelis), sample no. 24; F – Colomisphaera nagyi (Borza), sample no. 33; G – *Colomisphaera nagyi* (Borza), sample no. 34; H – *Ammobaculites,* sample no. 66; I – *Eomarssonella,* sample no. 103; J – *Reophax*, sample no. 149; K – Hexactinellid sponge, sample no. 166; L – *Terebella lapilloides* Münster sample no. 36; M – Hexactinellid sponge, sample no. 156; N – *Subnebrodites planula* close to the boundary between the Lar Fm. and K2 rock unit (lower Kimmeridgian); O – *Orthosphinctes* in the uppermost part of the Lar Fm. (lower Kimmeridgian)

scale bars: A–G – 50 μm; H–J, L –100 μm, K–M – 500 μm; A–E: Dalichai Fm., uppermost Oxfordian – lowest Kimmeridgian; F–M: Lar Fm., lower Kimmeridgian

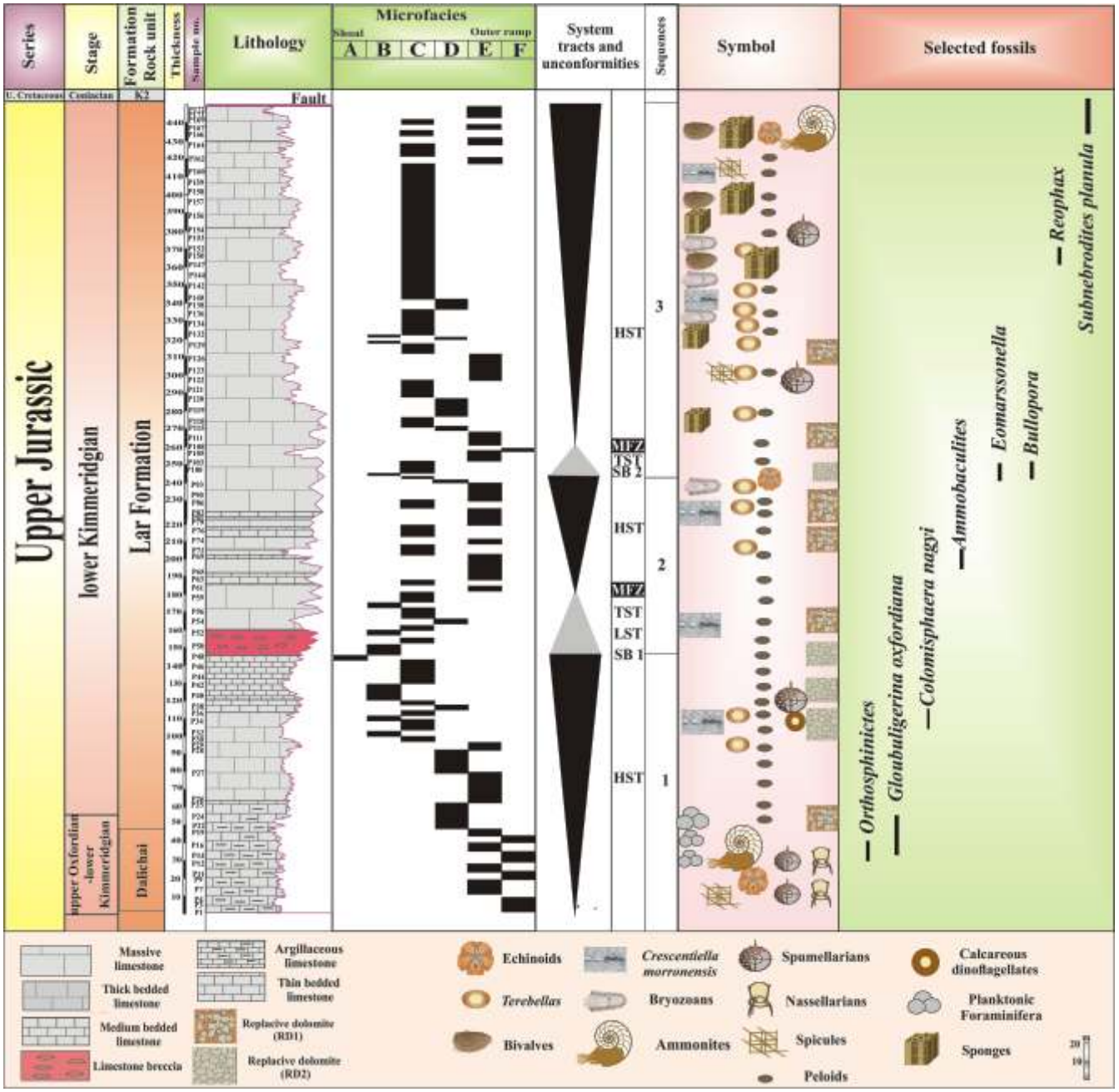

Fig. 6. Vertical distribution of microfacies and palaeoenvironmental and sequence-stratigraphic interpretation of the Lar Fm. at the Polur section of the Alborz Mountains, as well as distribution of index microfossils in the Lar Fm., Polur section

present in packstone to grainstone textures and contributing to microbial associations. *Crescentiella morronensis* in this microfacies show thinner walls (Fig. 8H, I), which implies increasing water depth (Leinfelder, 2001).

MF-E, BIOCLASTIC MUDSTONE TO WACKESTONE (OUTER RAMP)

These deposits developed as mudstones and bioclastic wackestones. Bioclastic elements include thin shells of brachiopods, bryozoan fragments and tubes of *Terebella*. Foraminifera including *Ammobaculites*, *Bullopora*, and *Eomarssonella* are observable within this microfacies (Fig. 7E). Hexactinellid sponges are present locally. This microfacies is most commonly observed in thick-bedded limestone. Because of the good preservation of the hexactinellid sponges within this microfacies, it may have formed in a low-energy basinal environment (Flügel, 2010).

MF-F, BIOCLASTIC RADIOLARIAN-RICH PELAGIC BIVALVE WACKESTONE TO PACKSTONE (OUTER RAMP)

This facies occupies the lower part of the section. Micrite matrix with common to abundant pelagic macrofossils (filaments, pelagic bivalves), skeletal elements of planktonic crinoids (*Saccocoma* sp.) and microfossils (calcified radiolarians,

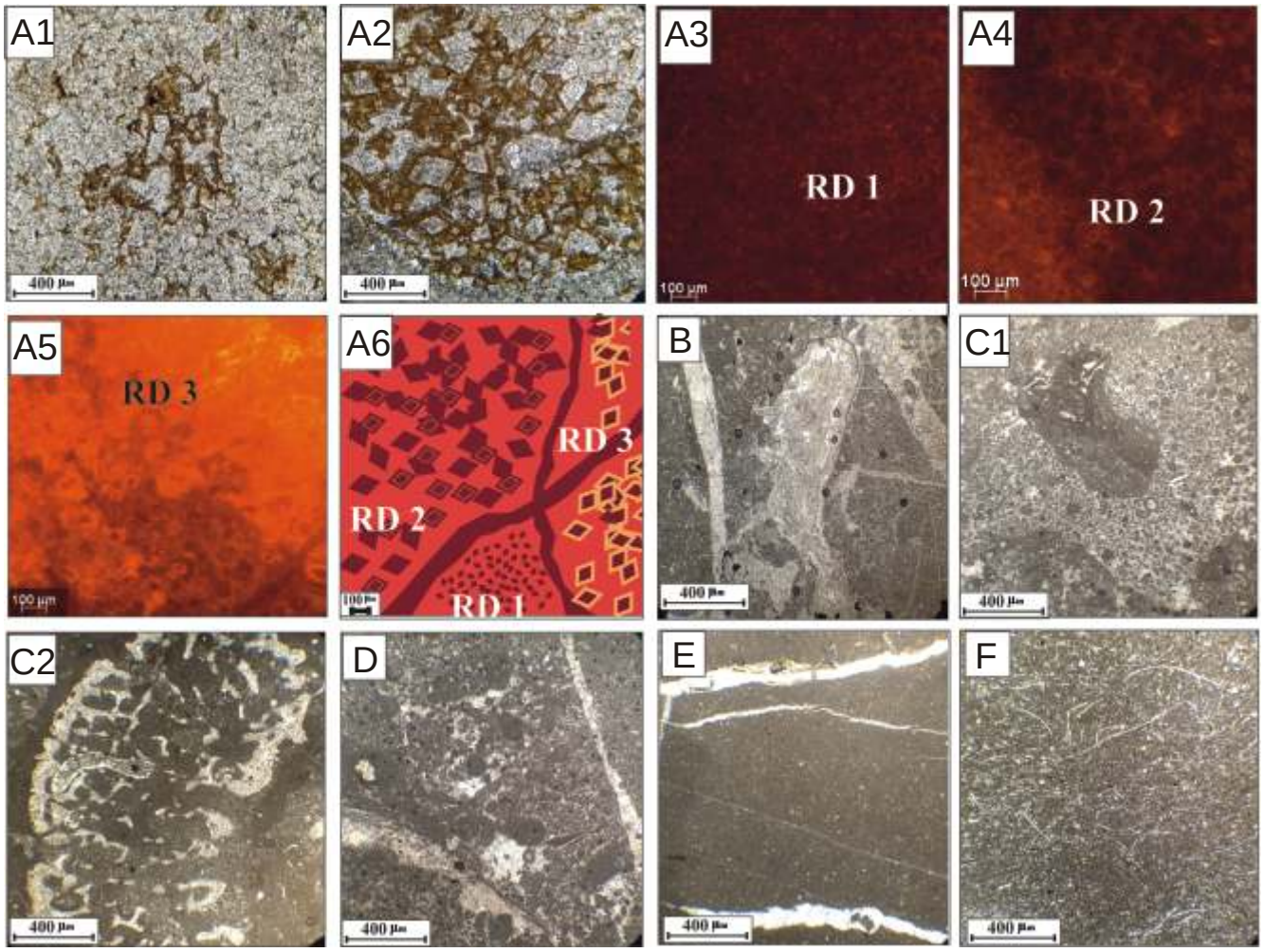

Fig. 7. The two depositional environments of the homoclinal ramp depositional system of the Lar Fm. in the Polur section (Fig. 1) and the six associated microfacies. The six microfacies are A1 – MF-A, dolomitic sparstone; A2 – MF-A, dolomitic sparstone; A3 – MF-A, cathodoluminescence (CL) image of Type-1 replacive dolomite (RD1) in the Lar Fm.; A4 – MF-A, Cathodoluminescence (CL) image of Type-2 replacive dolomite (RD2) in the Lar Fm.; A5 – MF-A, Cathodoluminescence (CL) image of Type-3 replacive dolomite (RD3) in the Lar Fm.; A6 – MF-A, a schematic representation of RD1, 2, 3 in the Lar Fm.; B – MF-B, an intraclastic bioclastic wackestone to packstone; C1 – MF-C, a bioclastic peloidal microbial *Crescentiella* packstone; C2 – MF-C, a bioclastic peloidal microbial *Crescentiella* packstone with sponges; D – MF-D, a bioclastic microbial peloidal packstone to grainstone; E – MF-E, a bioclastic mudstone to wackestone; F – MF-F, a bioclastic radiolarian-rich pelagic bivalve wackestone to packstone

sponge spicules, and planktonic foraminifera; Fig. 7F) are characteristic of this microfacies, while *Globuligerina oxfordiana* is one of the dominant microfossils. The lack of benthic fauna and the very dark colour of the thin-bedded and laminated mudstone indicate low-oxygen conditions on the seafloor where organic matter was preserved and bioturbation was absent.

Field observations illustrate very gradual vertical and lateral changes in the carbonate microfacies, thus implying gradual changes in palaeobathymetric relief (Burchette and Wright, 1992). In the absence of slumps and gravitational deposits, a homoclinal carbonate ramp model is proposed for the Polur section (Fig. 8).

DEPOSITIONAL SEQUENCES

Depositional sequences (DSs) were defined according to the approach described by Hunt and Tucker (1992, 1995), Strasser et al. (1999) and Catuneanu et al. (2011). In this conceptual sequence-stratigraphic model, a complete depositional sequence (DS) consists of a falling-stage systems tract (FSST), a lowstand systems tract (LST), a transgressive system tract (TST) and a highstand systems tract (HST). The six microfacies of the Lar Fm. were used to define stacking patterns. Three depositional sequences (DS) can be defined ranging in age from latest Oxfordian to early Kimmeridgian (Fig. 6). Upper bounding surfaces (sequence boundaries – SB) were delineated for each of DSs1–3 at the top of the HST. Lower bounding surfaces were observed at the base of the TST in all other cases. Nowhere was a FSST observed (Fig. 6). The absence of a FSST is due to a lack of sediment accumulation during relative sea- evel fall in forced regression (Bradshaw and Nelson, 2004). Here, maximum flooding zones (MFZs) were defined at the most distal facies instead of at maximum flooding surfaces (MFS) because no clear surfaces were exposed.

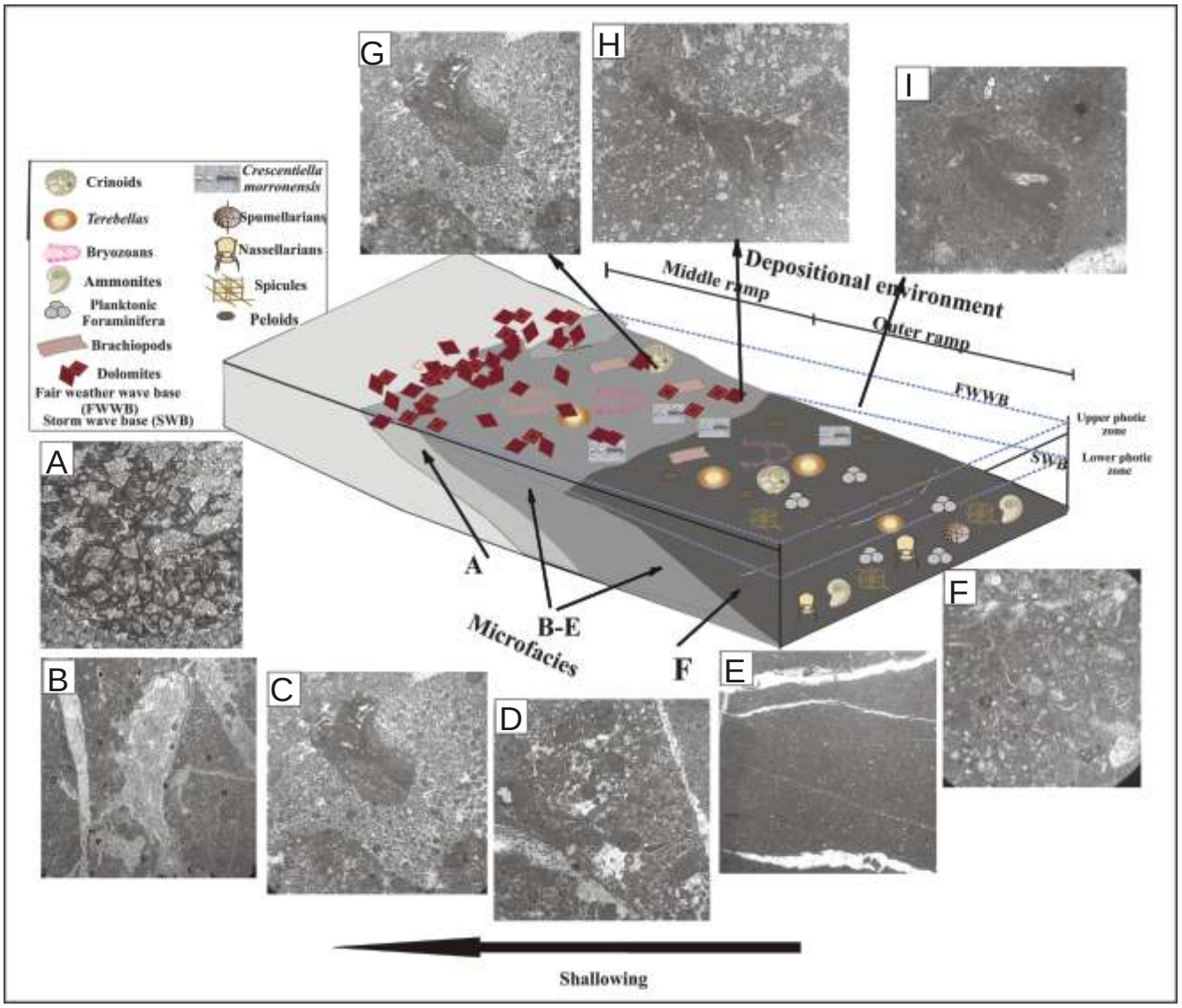

Fig. 8. The two depositional environments of the homoclinal ramp depositional system of the Lar Fm. in the Polur section and the six associated microfacies; A–F are recorded microfacies of Figures 7; G–I show changes in the *Crescentiella* thickness with depth

DEPOSITIONAL SEQUENCE 1

In the Polur section, the Lar Fm. overlies the Dalichai Fm. (Fig. 6), while in the areas adjacent to the Marghsoo section, it overlies the Shemshak Group. DS1 in the Polur section is represented only by its highstand deposits (HST). It comprises argillaceous limestone in its lower part (top of the Dalichai Fm.), passing into medium-to thick-bedded limestone in its upper part (Fig. 6). The vertical microfacies succession includes, in ascending order:

- bioclastic radiolarian-rich pelagic bivalve wackestone to packstone (MF F, outer ramp);
- bioclastic mudstone to wackestone (MF E, outer ramp);
- bioclastic microbial peloidal packstone to grainstone (MF D, middle ramp);
- bioclastic peloidal microbial *Crescentiell*a packstone (MF C, middle ramp);
- intraclastic bioclastic wackestone to packstone (MF B, middle ramp);
- dolomitic sparstone (MF A, middle ramp).

This evolution of microfacies implies shallowing-upwards depositional environments and consequently, is interpreted as a HST. The upper sequence boundary (SB) of DS1 is represented by a dolomitic sparstone (MF A, middle ramp).

DEPOSITIONAL SEQUENCE 2

DS2 is the thinnest depositional sequence of the Lar Fm. and consists of LST, TST and HST (Fig. 6). DS2 comprises breccia limestone and thick-bedded limestone in the lower part and thin- to bedded limestone to massive limestone in its upper part. The LST of DS2 consists of a breccia limestone with pieces of dolomitic sparstone (MF A, middle ramp), intraclastic bioclastic wackestone to packstone (MF B, middle ramp), and bioclastic peloidal microbial *Crescentiella* packstone (MF C, middle ramp). This indicates subaerial exposure and reworking of previously deposited sediment during a relative sea level fall. The TST is characterized by a deepening-upwards evolution of microfacies: bioclastic microbial peloidal packstone to grainstone (MF D, middle ramp), bioclastic peloidal microbial

Crescentiella packstone (MF C, middle ramp), intraclastic bioclastic wackestone to packstone (MF B), bioclastic peloidal microbial *Crescentiella* packstone (MF D, middle ramp) and bioclastic mudstone to wackestone (MF F, outer ramp). The maximum flooding zone (MFZ) is present at the top of the microfacies from bioclastic mudstone to wackestone (MF E), indicating an outer ramp depositional environment. The HST consists of bioclastic peloidal microbial *Crescentiella* packstone (MF C, middle ramp) and bioclastic mudstone to wackestone (MF E, outer ramp). The upper sequence boundary is characterized by intraclastic bioclastic wackestone to packstone (MF B, middle ramp) along with dolomites that are locally visible and reflect a sequence boundary at the top of DS2.

DEPOSITIONAL SEQUENCE 3

DS3 typically consists of massive limestone to thick-bedded limestone with two systems tracts (TST and HST). Intraclastic bioclastic wackestone to packstone (MF B, middle ramp) occurs at the lower sequence boundary of DS2 that separates DS2 and DS3 (Fig. 6).

The TST is commonly represented by bioclastic peloidal microbial *Crescentiella* packstone (MF C, middle ramp) and bioclastic mudstone to wackestone (MF E, outer ramp). The deepening upwards trend in depositional environments of the TST indicates an increase in relative sea level and accommodation space. The maximum flooding zone (MFZ) is marked by the occurrence of bioclastic radiolarian-rich pelagic bivalve wackestone to packstone (MF F, outer ramp). The HST consists of bioclastic mudstone to wackestone (MF E, outer ramp), bioclastic microbial peloidal packstone to grainstone (MF D, middle ramp) and bioclastic peloidal microbial *Crescentiella* packstone (MF C, middle ramp). The smallest-scale sedimentary cycles (genetically related units, fourth-or fifth-order eustatic cycles) of the upper part of DS3 are well-developed (Fig. 6) because of the large thickness of the HST and consist of bioclastic peloidal microbial *Crescentiella* packstone (MF C, middle ramp), and bioclastic mudstone to wackestone (MF E, outer ramp). The fourth- or fifth-order eustatic cycles and HST of DS3 are cut by a fault corresponding to a regional orogeny that marks an important erosional phase and pervasive epigenetic karstification, as well as a tectonic phase, such as the Late Cimmerian orogeny, possibly related to fault movements that may have removed part of the HST rocks (Shahidi et al., 2008).

The oldest strata of the K2 rock unit (Upper Cretaceous) are at the top of the Lar Fm. The youngest strata of the Lar Fm. and the oldest strata of the K2 rock unit are separated by a major fault in this area (Fig. 4).

DISCUSSION

PALAEOBIOGEOGRAPHY

Upper Jurassic deposits formed during a long-term 1st-order rise in global sea level due to rifting in the central Atlantic (Gerdes et al., 2010). The sea level rise reached its Jurassic maximum during Kimmeridgian time. A major Late Jurassic seaway opened during rifting in the central Atlantic, connecting the central Atlantic with the central Neo-Tethys. The palaeolatitude of the Polur area of the central Alborz Zone in the central Neo-Tethys was ~30°N during the Late Jurassic and rifting in the central Atlantic was at ~24°N, which would have led to the exchange of calcareous dinoflagellates through a seaway between the central Atlantic and the Alborz Zone (Daneshian and Saleh, 2020). In the Polur area studied, the calcareous dinoflagellate cysts *Colomisphaera nagyi* were observed. In Iran, calcareous dinoflagellates of Late Jurassic age have been recorded from the Lar Fm., Marghsoo section, central Alborz Zone, where Daneshian and Saleh (2020) found *Colomisphaera fibrata*, *Cadosina parvula*, *Stomiosphaera moluccana*, *Cadosina semiradiata semiradiata*, *Colomisphaera tenuis* and *C. fortis*. The distribution of calcareous dinoflagellates in the Upper Jurassic here resembles that of the adjacent subbasins (Daneshian and Saleh, 2020) and that of the European and Mediterranean regions, demonstrating connection between the central Atlantic and the Neo-Tethys Ocean. Such connected basins have led to the same biological zones commonly used in age determination from the upper Oxfordian to the upper Kimmeridgian in the Neo-Tethys Ocean region (Daneshian and Saleh, 2020). So far, calcareous dinoflagellates have not been known from south-west Iran (Zagros); therefore, there was no faunal relationship with south-west Iran (Zagros) throughout the Jurassic Period, suggesting that wide and deep oceanic areas in fact formed physical barriers for calcareous dinoflagellate dispersal.

PALAEOECOLOGY

MICRO-ENCRUSTER ASSOCIATIONS

Terebella-Crescentiella associations are commonly observed in the Upper Jurassic deposits of the northern Neo-Tethys shelf (e.g., Leinfelder et al., 1996; Kowal-Kasprzyk et al., 2020). Such *Terebella-Crescentiella* associations were identified throughout the Lar Fm. (Fig. 7C1, C2, D) and within MF–C (bioclastic peloidal microbial *Crescentiella* packstone to grainstone) and MF–D (bioclastic microbial peloidal packstone to grainstone). *Terebella lapilloides* reflects a low-energy setting under dysoxic conditions (e.g., Reolid et al., 2005; Kaya and Altiner, 2014). The presence of microbialites and *Crescentiella* in thick massive limestone indicates palaeodepths between the fair-weather and the storm wave bases, i.e., around 40–60 m (e.g., Leinfelder et al., 1996; Krajewski, 2000), and a nutrient-rich (eutrophic) environment (Kowal-Kasprzyk et al., 2020).

FORAMINIFERAL ASSEMBLAGES

Foraminiferal abundance throughout the Lar Fm. is low. Larger agglutinated foraminifera rarely occur in the Lar Fm. while smaller agglutinated foraminifera are more common (Aghaei et al., 2012; Kochhann et al., 2015). The foraminiferal assemblages of the Lar Fm. are strongly dominated by r-selected strategists and agglutinated foraminiferal taxa. Morphogroups of agglutinated foraminifera are commonly used as indicators of palaeobathymetry and/or organic carbon flux (Jones and Charnock, 1985; Kaminski and Kuhnt, 1995; Reolid et al., 2010; Smoleń, 2012). Here, the agglutinated foraminifera recorded were arranged into one morphogroup according to Cetean et al. (2011). This morphogroup comprises elongated shapes with a supposed infaunal mode of life and of small size,

here represented by *Ammobaculites*, *Eomarssonella*, and *Reophax* (Fig. 5H–J). The dominance of r-selected strategists among benthic foraminifera suggests stressful palaeoenvironmental conditions, probably related to low bottom-water oxygen levels (Kochhann et al., 2015). The low diversity of planktonic foraminifera is reminiscent of r-strategists (opportunistic species), which indicates eutrophic conditions. This assemblage is numerically dominated by simple test morphotypes such as *Globuligerina oxfordiana*. A dominance of simple test morphotypes in the Jurassic deposits has previously been widely recorded in Neo-Tethys successions (Gradstein et al., 2017).

HEXACTINELLID SPONGES

Hexactinellid sponges are present throughout the upper part of the Lar Fm. (Fig. 5M, K). These are sponges with siliceous triaxon hexactine spicules or derivatives of that basic form (Flügel, 2010). Organisms associated with hexactinellid sponges in the Lar Fm. include mainly foraminifera, brachiopods, bryozoans and echinoderms. Hexactinellid sponges from different depositional environments reflecting different hydrodynamic regimes are preserved differently (Brachert, 1991). Preservation of hexactinellid sponges is best in low-energy basinal carbonates due to slow silica dissolution (Flügel, 2010). Portions of the northern shelf of the Neo-Tethys where the Alborz Zone is located may have been a favourable place for the upwelling of hypoxic waters (Conway et al., 2017). The occurrence of hexactinellid sponges in the ramp environment of the Lar Fm. is consistent with such oceanic conditions. Leinfelder et al. (1994) considered that hexactinellid sponges can live on a broad low-slope shelf within a stratified ocean marked by sluggish water circulation.

REGIONAL DEPOSITIONAL SEQUENCES

The relative stratigraphic positions of DSs 1–3 and sequence boundaries in the uppermost Oxfordian to the lower Kimmeridgian (Fig. 9A, B) of the Polur area show a fair match to the late Oxfordian to early Kimmeridgian sequences (JOx7, JOx8, JKi1, and JKi2) on the Haq (2018) global sea level curve (Fig. 9A, B). The similar relative positions of most of the Polur area sequence boundaries to those of the Haq (2018) global chart suggest that global eustasy may have influenced the timing of Kimmeridgian sequence boundaries here (Fig. 9A, B). MFSs identified during the depositional sequences of JOx7, JOx8, JKi1 and JKi2 reflect the most regionally correlatable transgressions, having been identified throughout southern Europe and North Africa (Atrops and Benest, 1984; Zappaterra, 1994), along the eastern edge of the Arabian Shelf (Rousseau et al., 2005) and in the Interior Fars province of Iran (Golestaneh, 1965). Regional tectonic subsidence combined with an overall increase in eustatic signatures led to the extensive deposition on ramps throughout the Neo-Tethys (Gerdes et al., 2010). During the Kimmeridgian, deposition on parts of the central Neo-Tethys was similar to that in the western Neo-Tethys and other regions globally and was characterized by high accommodation space and high sediment volumes, which led to very thick 3rd-order depositional sequences in the Polur section (Fig. 9B). During the late Oxfordian to early Kimmeridgian, the Alborz Zone central Neo-Tethys was in a platform, ramp, and anoxia basinal depositional setting similar to the western Neo-Tethys. The uppermost DS3 in the Polur section has been cut out by a fault at the top of DS3. It is likely that tectonics may have played a role in influencing the termination of the Lar Fm. and Kimmeridgian succession. The presence of a major fault and a large number of fractures at the top of the Lar Fm. is attributed to the early stages of the Late Cimmerian orogeny (Fig. 4), which led to major unconformity and produced many faults and karstification in the Polur area. The Cimmerian unconformity also appears to correlate with a major regional unconformity in Iran (Aghanabati, 2004), with a sea level fall on the Arabian Plate recorded by Sharland et al. (2004), and the sea level fall recorded in Neo-Tethys Mesozoic carbonates as described by Gerdes et al. (2010). Evidence of rapid alternations of sub-aerial exposure and complete submergence on platform surfaces indicates tectonic instability and/or eustatic fluctuations during this time (Bádenas and Aurell, 2001; Benito et al., 2005).

CONCLUSIONS

Based on the analysis of 173 thin-sections and on micropalaeontological, biostratigraphic and sequence-stratigraphic investigations, the following conclusions may be presented for the Lar Fm. in the Polur area:

1. Four genera of benthic foraminifera (*Ammobaculites*, *Bullopora, Eomarssonella*, *Reophax*), one species of planktonic foraminifera (*Globuligerina oxfordiana*), one species of calcareous dinoflagellate (*Colomisphaera nagyi*), one ammonite genus (*Orthosphinctes*), and one ammonite species (*Subnebrodites planula*) have been identified.
2. The age of the Lar Fm. in the Polur area is uppermost Oxfordian-lowest Kimmeridgian at the base and lower Kimmeridgian at the top of the formation, based on foraminifera, ammonites and calcareous dinoflagellates.
3. Six microfacies (MF) are defined and attributed to depositional environments: dolomitic sparstone (MF-A, middle ramp); intraclastic bioclastic wackestone to packstone (MF-B, middle ramp); bioclastic peloidal microbial Crescentiella packstone (MF-C, middle ramp); bioclastic microbial peloidal packstone to grainstone (MF-D, middle ramp); bioclastic mudstone to wackestone (MF-E, outer ramp); bioclastic radiolarian-rich pelagic bivalve wackestone to packstone (MF-F, outer ramp).
4. Three Late Jurassic depositional sequences are delineated based on microfacies variations. The HST of DS1 represents a rapidly upwards shallowing succession that indicates a shift from an outer ramp to middle ramp depositional setting. The LST of DS2 consists of a breccia limestone with patches of dolomitic sparstone, which indicates subaerial exposure and reworking of previously deposited sediment due to a relative sea level fall. The HST of DS3 is truncated by a fault corresponding to a regional tectonic phase related to the Late Cimmerian orogeny. This resulted in erosion and pervasive epigenetic karstification.
5. Foraminiferal assemblages and hexactinellid sponges reflect stressful palaeoenvironmental conditions, probably related to low oxygen levels. These are attributed to eutrophic conditions prevailing during deposition of the Lar Fm.

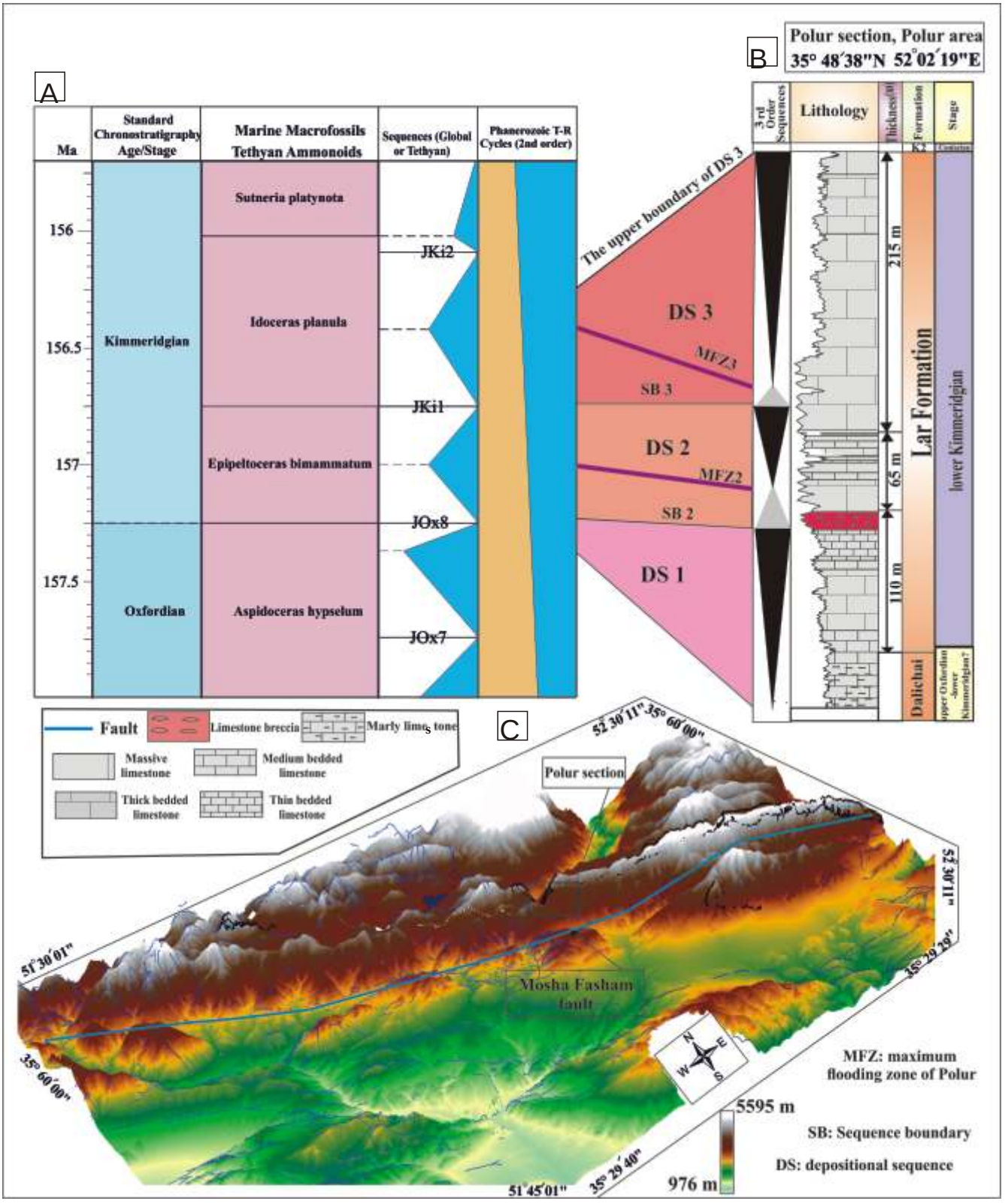

Fig. 9A – a chart of Tethyan ammonoid zones, 2rd and 3rd sequences of global sea level after Haq (2018); B – lithological columns of the Polur sections, Central Alborz Mountains, north of Iran; C – DEM of the central Alborz Mountains with location of selected sections; note the change in elevation created by the Mosha Fasham Fault and strong epigenic karstification in the central Alborz Mountains along this fault (for further information see Allen et al., 2003; Shahidi et al., 2008)

Acknowledgments. The authors would like to thank Kharazmi University for supporting this research. We appreciate the support of J. Daneshian and his thoughtful comments. The authors are grateful to A. Raoufian, H. Parent, and A. Wierzbowski for providing some of the ammonite's identification and their constructive comments. We also thank F. Gradstein for his guidance. The manuscript benefitted from careful reviews by A. Strasser, J. Grabowski, J. Smoleń and an Anonymous reviewer. We appreciate the assistance of E. Rooshanpour, M. Esmaeilzadeh, L. Delfan, A. Hasan Nezhad, S. Sayadi, and H. Mousavi in the fieldwork.

REFERENCES

Aghaei, A., Mahboubi, A., Mousavi-Harami, R., Heubeck, C., Nadjafi, M., 2012. Facies analysis and sequence stratigraphy of an Upper Jurassic carbonate ramp in the Eastern Alborz range and Binalud Mountains, NE Iran. Facies, **58**: 1–27. https://doi.org/10.1007/s10347-012-0339-8

Aghanabati, A., 2004. Geology of Iran. Geological Survey of Iran, Tehran.

Aghanabati, A., Rezaie, A., 2009. Stratigraphic Chart of Iran. Geological Survey of Iran, Tehran.

Allen, M.B., Ghassemi, M.R., Shahrabi, M., Qorashi, M., 2003. Accommodation of late Cenozoic oblique shortening in the Alborz range, northern Iran. Journal of Structural Geology, **25**: 659–672. https://doi.org/10.1016/S0191-8141(02)00064-0

Assereto, R., 1966. Geological Map of Upper Djadjerud and Lar Valleys (Central Alborz, Iran) with explanatory Notes. Istituto di Geologia, Universitá di Milano Serie G, pubblicazione.

Atrops, F., Benest, M., 1984. Découverte de faunes d'Ammonites de la zone à Platynota (Kimméridgien inférieur) dans les Monts de Chellala (avant-pays Tellien, Algérie); Conséquences stratigraphiques et paléogéographiques. Geobios, **15**: 951–1057. https://doi.org/10.1016/S0016-6995(82)80041-7

Bádenas, B., Aurell, M., 2001. Kimmeridgian paleogeography and basin evolution of north eastern Iberia. Palaeogeography, Palaeoclimatology, Palaeoecology, **168**: 291–310. https://doi.org/10.1016/S0031-0182(01)00204-8.

Bakhmutov, V.G., Halásová, E., Ivanova, D.K., Józsa, Š., Reháková, D., Wimbledon, W.A.P., 2018. Biostratigraphy and magnetostratigraphy of the uppermost Tithonian–Lower Berriasian in the Theodosia area of Crimea (southern Ukraine). Geological Quarterly, **62** (2): 197–236. https://doi.org/10.7306/gq.1404

Barrier, E., Vrielynck, B., 2008. Palaeotectonic maps of the Middle East, in tectono sedimentary–palinspastic maps from Late Norian to Piacenzian. Commission for the Geological Map of the World/UNESCO.

Benito, M.I., Lohmann, C.K., Mas, R., 2005. Late Jurassic paleogeography and paleoclimate in the northern Iberian Basin of Spain: constraints from diagenetic records in reefal and continental carbonates. Journal of Sedimentary Research, **75**: 82–96. https://doi.org/10.2110/jsr.2005.008

Bochud, M., 2011. Tectonics of the Eastern Greater Caucasus in Azerbaijan. Ph.D. Thesis, University of Fribourg, Fribourg, Switzerland.

Brachert, T., 1991. Environmental control on fossilization and siliceous sponge assemblages : ŕ proposal. In: Fossil and Recent Sponges (eds. J. Reitner and H. Keupp): 543–553. Berlin (Springer). https://doi.org/10.1007/978-3-642-75656-6_45

Bradshaw, B., Nelson, C., 2004. Anatomy and origin of autochthonous late Pleistocene forced regression deposits, east Coromandel inner shelf, New Zealand: implications for the development and definition of the regressive systems tract. New Zealand. Journal of Geology and Geophysics, **47**: 81–99. https://doi.org/10.1080/00288306.2004.9515039

Burchette, T.P., Wright, V.P., 1992. Carbonate ramp depositional systems. Sedimentary Geology, **10**: 3–57. https://doi.org/10.1016/0037-0738(92)90003-A

Catuneanu, O., Galloway, W.E., Kendall, C.G.St.C., Miall, A.D., Posamentier, H.W., Strasser, A., Tucker, M.E., 2011. Sequence stratigraphy: methodology and nomenclature. Newsletters on Stratigraphy, **44**: 173–245. http://dx.doi.org/10.1127/0078-0421/2011/0011

Cetean, C.G., Bălc, R., Kaminski, M.A., Filipescu, S., 2011. Integrated biostratigraphy and palaeoenvironments of an upper Santonian – upper Campanian succession from the southern part of the Eastern Carpathians, Romania. Cretaceous Research, **32**: 575–590. https://doi.org/10.1016/j.cretres.2010.11.001

Conway, K.W., Whitney, F., Leys, S.P., Barrie, J.V., Krautter, M., 2017. Sponge reefs of the British Columbia, Canada Coast: impacts of climate change and ocean acidification. In: Climate Change, Ocean Acidification and Sponges (eds. J. Carballo and J. Bell): 429–445. Springer International Publishing AG. https://doi.org/10.1007/978-3-319-59008-0_10

Daneshian, J., Saleh, Z., 2020. Marine faunal microfossils from Late Jurassic to Late Cretaceous of the Central Neo-Tethys: A case study from the central Alborz, Iran. Marine Micropaleontology, **156**: 101856. https://doi.org/10.1016/j.marmicro.2020.101856

Daneshian, J., Saleh, Z., Swennen, R., Mosaddegh, H., 2021. Porosity development in central Alborz Upper Jurassic deposits (N-Iran): sequence stratigraphy, diagenesis and mechanical Stratigraphy. Neues Jahrbuch für Geologie und Paläontologie Abhandlungen, **300**: 117–143. 10.1127/njgpa/2021/0975

Dunham, R.J., 1962. Classification of carbonate rocks according to depositional texture. AAPG Memoirs, **1**: 108–121. https://doi.org/10.1306/M1357

Embry, A.F., Klovan, J.E., 1971. A Late Devonian reef tract on northeastern Banks Island N.W.T. Bulletin of Canadian Petroleum Geology, **19**: 730–781. https://doi.org/10.35767/gscpgbull.19.4.730

Fathi, S., Mosaddegh, H., 2012. The study of diagenetic effects on Jurassic dolomitic limestone host rocks in Ahvano Pb-Zn deposits, North Damghan, Iran. Petrology Journal of the University of Isfahan, **2**: 85–98.

Flügel, E., 2010. Microfacies of Carbonate Rocks. Springer, Berlin. https://doi.org/10.1007/978-3-642-03796-2

Gerdes, K.D., Winefield, K.D.P., Simmons, M.D., Van Oosterhout, C., 2010. The influence of basin architecture and eustacy on the evolution of Tethyan Mesozoic and Cenozoic carbonate sequences. Geological Society Special Publications, **329**: 9–41. https://doi.org/10.1144/SP329.2

Golestaneh, A., 1965. A micropaleontological study of the Upper Jurassic and Lower Cretaceous of southern Iran. Ph.D. Thesis, University of London.

Gradstein, F., Gale, A., Kopaevich, L., Waskowska, A., Grigelis, A., Glinskikh, L., Gorog, A., 2017. The planktonic foraminifera of the Jurassic. Part II: stratigraphy, palaeoecology and palaeobiogeography. Swiss Journal of Palaeontology, **136**: 259–271. https://doi.org/10.1007/s13358-017-0132-y

Haq, B.U., 2018. Jurassic sea-level variations: a reappraisal. GSA Today, **28**: 4–10. 10.1130/GSATG359A.1

Hunt, D., Tucker, M.E., 1992. Stranded parasequences and the forced regressive wedge systems tract: deposition during base-level fall. Sedimentary Geology, **81**: 1–9. https://doi.org/10.1016/0037-0738(92)90052-S

Hunt, D., Tucker, M.E., 1995. Stranded parasequences and the forced regressive wedge systems tract: deposition during base level fall – reply. Sedimentary Geology, **95**: 147–160. https://doi.org/10.1016/0037-0738(94)00123-C

Ivanova, D., Kołodziej, B., Koleva-Rekalovai, E., Roniewicz, E., 2008. Oxfordian to Valanginian palaeoenvironmental evolution on the western Moesian Carbonate Platform: a case study from SW Bulgaria. Annales Societatis Geologorum Poloniae, **78**: 65–90.

Jones, R.W., Charnock, M.A., 1985. "Morphogroups" of agglutinated foraminifera. Their life position and feeding habits and potential applicability in (paleo)ecological studies. Revue de Paléobiologie, **4**: 311–320.

Kaminski, M.A., Kuhnt, W., 1995. Tubular agglutinated foraminifera as indicators of organic carbon flux. Grzybowski Foundation Special Publication, **3**: 141–144.

Kaya, M.Y., Altiner, D., 2014. *Terebella lapilloides* Munster, 1833 from the Upper Jurassic–Lower Cretaceous Inalti carbonates, northern Turkey: its taxonomic position and paleoenvironmental-paleoecological significance. Turkish Journal of Earth Sciences, **23**: 166–183. https://doi.org/10.3906/yer-1306-2

Kırmacı, M.Z., 2013. Origin of dolomite in the Late Jurassic platform carbonates, Bolkar Mountains, Central Taurides, Turkey: petrographic and geochemical evidence. Geochemistry, **73**: 383–398. https://doi.org/10.1016/j.chemer.2012.11.001

Kochhann, K.G.D., Bergue, C.T., Falahatgar, M., Javidan, M., Parent, H., 2015. Benthic foraminifera and ostracoda from the Dalichai Formation (Aalenian–Bajocian) at Telma-Dareh, Alborz Mountain, Northern IRAN. Revista Brasiliera de Paleontologia, **18**: 3–20.

Kowal-Kasprzyk, J., Krajewski, M., Gedl, P., 2020. The oldest stage of the Outer Carpathian evolution in the light of Oxfordian–Kimmeridgian exotic clast studies (southern Poland). Facies, **66**: 2. https://doi.org/10.1007/s10347-020-0595-y

Krajewski, M., 2000. Lithology and morphology of Upper Jurassic carbonate buildups in the Będkowska Valley, Kraków region, Southern Poland. Annales Societatis Geologorum Poloniae, **70**:51–163.

Kuznetsova, K.I., Grigelis, A., Adjamian, J., Jarmakani, E., Hallaq, L., 1996. Zonal Stratigraphy and Foraminifera of the Tethyan Jurassic (Eastern Mediterranean). Gordon and Breach Science Publishers, Amsterdam.

Leinfelder, R.R., Krautter, K., Laternser, R., Nose, M., Schmid, D.U., Schwiegert, G., Werner, W., Keupp, H., Brugger, H., Herrman, R., Rehfeld-Kiefer, U., Schroeder, J.H., Reinhold, C., Koch, R., Zeiss, A., Schweizer, V., Christmann, H., Menges, G., Luterbacher, H., 1994. The origin of Jurassic reefs: current research and results. Facies, **31**: 1–56. https://doi.org/10.1007/BF02536932

Leinfelder, R.R., Werner, W., Nose, M., Schmid, D.U., Krautter, M., Laternser, R., Takacs, M., Hartmann, D., 1996. Paleoecology, growth parameters and dynamics of coral, sponge and microbolite reefs from the Late Jurassic. Göttinger Arbeiten zur Geologie und Paläontologie, **2**: 227–248.

Leinfelder, R.R., 2001. Jurassic reef ecosystems. Topics in Geobiology, **17**: 251–309. https://doi.org/10.1007/978-1-4615-1219-6_8

Loeblich, A.R., Tappan, H., 1988. Foraminiferal Genera and their Classification: New York, Van Nostrand, **1**: 970. https://doi.org/10.1007/978-1-4899-5760-3

Majidifard, M.R., 2008. Lithostratigraphy and sedimentary environment of the Dalichai and Lar formations (Middle-Upper Jurassic) of NNE Iran. Geoscience, **17**: 94–114.

Moliner, L., Olóriz, F., 2009. Updated biostratigraphy of Jurassic (lower Kimmeridgian) deposits containing the ammonite Ataxioceras from the eastern Iberian Range, northeastern Spain. GFF, **131**: 195–203. https://doi.org/10.1080/11035890902952886

Muttoni, G., Gaetani, M., Kent, D.V., Sciunnach, D., Angiolini, L., Berra, F., Garzanti, E., Mattei, M., Zanchi, A., 2009. Opening of the Neo-Tethys Ocean and the Pangea B to Pangea A transformation during the Permian. Geoarabia, **14**: 17–46. https://doi.org/10.2113/geoarabia140417

Naderi, E., 2002. Microfacies, sedimentary environment and sequences of the Dalichai and Lar Formation. MSc. Thesis, Kharazmi University, Tehran.

Nagy, J., Hendrickson, R.M.S., 2022. Hyposaline to hypoxic foraminiferal facies and stratigraphy of Middle Jurassic to basal Cretaceous deposits of the Trřndelag Platform, mid-Norwegian shelf. Palaeogeography, Palaeoclimatology, Palaeoecology, **589**: 110831. https://doi.org/10.1016/j.palaeo.2022.110831

Ogg, J.G., Ogg, G., Gradstein, F.M., 2016. A Concise Geologic Time Scale. Elsevier, USA. https://doi.org/10.1016/C2009-0-64442-1

Reháková, D., 2000a. Evolution and distribution of the Late Jurassic and Early Cretaceous calcareous dinoflagellates recorded in the Western Carpathian pelagic carbonate facies. Mineralia Slovaca, **32**: 79–88.

Reháková, D., 2000b. Calcareous dinoflagellate and calpinellid bioevents versus sea-level fluctuations recorded in the West-Carpathian (Late Jurassic/Early Cretaceous) pelagic environments. Geologica Carpathica, **51**: 229–243.

Reháková, D., Matyja, B., Wierzbowski, A., Schlögl, J., Krobicki, M., Barski, M., 2011. Stratigraphy and microfacies of the Jurassic and lowermost Cretaceous in the Veliky Kamenets section (Pieniny Klippen Belt, Carpathians, Western Ukraine). Volumina Jurassica, **9**: 61–104.

Reolid, M., Gaillard, C.h., Olóriz, F., Rodríguez-Tovar, F.J., 2005. Microbial encrustations from the Middle Oxfordian-earliest Kimmeridgian lithofacies in the Prebetic Zone (Betic Cordillera, southern Spain): characterization, distribution and controlling factors. Facies **50**: 529–543. https://doi.org/10.1007/s10347-004-0030-9

Reolid, M., Nagy J., Rodriguez-Tovar, F.J., 2010. Ecostratigraphic trends of Jurassic agglutinated foraminiferal assemblages as a response to sea-level changes in shelf deposits of Svalbard (Norway). Palaeogeography, Palaeoecology, Palaeoclimatology, **293**: 184–196. https://doi.org/10.1016/j.palaeo.2010.05.019

Rousseau, M., Dromart, G., Garcia, J.-P., Atrops, F., Guillocheau, F., 2005. Jurassic evolution of the Arabian carbonate platform edge in central Oman Mountains. Journal of the Geological Society of London, **162:** 1–14. https://doi.org/10.1144/0016-764903-178

Sarfi, M., Yazdi-Moghadam, M., 2016. Stratigraphy of the Upper Jurassic shallow marine carbonates of the Moghan area (NW Iran), with paleobiogeography implication on *Alveosepta jaccardi* (Schrodt, 1894). Geopersia, **6**: 187–196.

Schweigert, G., Kuschel, H., 2017. Comments on the identification of Ammonites planula Hehl in Zieten, 1830 (Upper Jurassic, SW Germany). Volumina Jurassica, **15**: 1–15. https://doi.org/10.5604/01.3001.0010.3920

Seyed-Emami, K., Schairer, G., Zeiss, A., 1995. Ammoniten aus der Dalichai-Formation (Mittlerer bis Oberer Jura) und der Lar-Formation (Oberer Jura) N Emamzadeh Hashem (Zentrala-lborz, Nordiran). Mitteilungen der Bayerischen Staatssammlung für Paläontologie und historische Geologie, **35**: 39–52.

Sharland, P.R., Casey, D.M., Davies, R.B., Simmons, M.D., Sutcliffe, O.E., 2004. Arabian Plate Sequence Stratigraphy revisions to SP2. GeoArabia, **9**: 199–214. https://doi.org/10.2113/geoarabia0901199

Shahidi, A., Barrier., E., Brunet, M.F., Saidi, A., 2008. Tectonic evolution and Late Triassic- Middle Eocene extension in central Alborz, Iran. Geoscience, **17**: 4–25. https://doi.org/10.22071/gsj.2011.54384

Smoleń, J., J., 2012. Faunal dynamics of foraminiferal assemblages in the Bathonian (Middle Jurassic) ore-bearing clays at

Gnaszyn, Kraków-Silesia Homocline, Poland. Acta Geologica Polonica, **62**: 403–419. https://doi.org/10.2478/v10263-012-0023-x

Stöcklin, J., 1968. Structural history and tectonics of Iran: a review. AAPGs Bulletin, **52**: 1229–1258. https://doi.org/10.1306/5D25C4A5-16C1-11D7-8645000102C1865D

Strasser, A., Pittet, B., Hillgärtner, H., Pasquier, J.B., 1999. Depositional sequences in shallow carbonate-dominated sedimentary systems: concepts for a high-resolution analysis. Sedimentary Geology, **128**: 201–221. https://doi.org/10.1016/S0037-0738(99)00070-6

Vahdati-Daneshmand, F., 1997. Geological map of east of Tehran. Scale 1:100 000, no. 6361. Geological Survey of Iran, Tehran.

Wilson, J.L., 1975. Carbonate Facies in Geologic History. Springer, New York. https://doi.org/10.1007/978-1-4612-6383-8

Wright, V.P., 1992. A revised classification of limestones. Sedimentary Geology, **76**: 177–185. https://doi.org/10.1016/0037-0738(92)90082-3

Zanchi, A., Berra, F., Mattei, M., Ghassemi, M., Sabouri, J., 2006. Inversion tectonics in Central Alborz, Iran. Journal of Structural Geology, **28**: 2023–2037. https://doi.org/10.1016/j.jsg.2006.06.020